Radiotherapy and Oncology 154 (2021) 292–298

Contents lists available at ScienceDirect

Radiotherapy and Oncology

journal homepage: www.thegreenjournal.com

Original Article

The tubarial salivary glands: A potential new organ at risk for radiotherapy

Matthijs H. Valstar [a,b,*], Bernadette S. de Bakker [c], Roel J.H.M. Steenbakkers [d], Kees H. de Jong [c], Laura A. Smit [e], Thomas J.W. Klein Nulent [f,g], Robert J.J. van Es [f,g], Ingrid Hofland [h], Bart de Keizer [i], Bas Jasperse [j], Alfons J.M. Balm [a,b], Arjen van der Schaaf [d], Johannes A. Langendijk [d], Ludi E. Smeele [a,b], Wouter V. Vogel [k,l]

[a] Dept. of Head and Neck Oncology and Surgery, The Netherlands Cancer Institute (NCI); [b] Dept. of Oral and Maxillofacial Surgery, Amsterdam UMC (AUMC); [c] Dept. of Medical Biology, Section Clinical Anatomy & Embryology, AUMC, University of Amsterdam, Amsterdam; [d] Dept. of Radiation Oncology, University of Groningen, University Medical Center Groningen (UMCG), Groningen; [e] Dept. of Pathology, NCI, Amsterdam; [f] Dept. of Head and Neck Surgical Oncology, UMC Utrecht Cancer Center (UMCU), University Medical Center Utrecht; [g] Dept. of Oral and Maxillofacial Surgery, UMCU, Utrecht; [h] Core Facility Molecular Pathology & Biobanking, Division of Pathology, NCI, Amsterdam, the Netherlands; [i] Dept. of Radiology and Nuclear Medicine, UMCU, Utrecht; [j] Dept. of Radiology; [k] Dept. of Nuclear Medicine; and [l] Dept. of Radiation Oncology, NCI, Amsterdam, the Netherlands

ARTICLE INFO

Article history:
Received 21 June 2020
Received in revised form 15 September 2020
Accepted 16 September 2020
Available online 23 September 2020

Keywords:
Tubarial glands
Salivary glands
Radiation toxicity
Radiotherapy
Head and neck cancer
PSMA PET/CT

ABSTRACT

Introduction: The presence of previously unnoticed bilateral macroscopic salivary gland locations in the human nasopharynx was suspected after visualization by positron emission tomography/computed tomography with prostate-specific membrane antigen ligands (PSMA PET/CT). We aimed to elucidate the characteristics of this unknown entity and its potential clinical implications for radiotherapy.

Materials and methods: The presence and configuration of the PSMA-positive area was evaluated in a retrospective cohort of consecutively scanned patients with prostate or urethral gland cancer (n = 100). Morphological and histological characteristics were assessed in a human cadaver study (n = 2). The effect of radiotherapy (RT) on salivation and swallowing was retrospectively investigated using prospectively collected clinical data from a cohort of head-neck cancer patients (n = 723). With multivariable logistic regression analysis, the association between radiotherapy (RT) dose and xerostomia or dysphagia was evaluated.

Results: All 100 patients demonstrated a demarcated bilateral PSMA-positive area (average length 4 cm). Histology and 3D reconstruction confirmed the presence of PSMA-expressing, predominantly mucous glands with multiple draining ducts, predominantly near the torus tubarius. In the head-neck cancer patients, the mean RT dose to the gland area was significantly associated with physician-rated post-treatment xerostomia and dysphagia $\geq$ grade 2 at 12 months (0.019/gy, 95%CI 0.005–0.033, p = .007; 0.016/gy, 95%CI 0.001–0.031, p = .036). Follow-up at 24 months had similar results.

Conclusion: The human body contains a pair of previously overlooked and clinically relevant macroscopic salivary gland locations, for which we propose the name tubarial glands. Sparing these glands in patients receiving RT may provide an opportunity to improve their quality of life.

The salivary gland system, with its three paired major glands and roughly 1000 minor glands spread throughout the aerodigestive tract submucosa, has been described in detail [1–4]. Its serous, mucous or mixed exocrine acini produce the saliva required for mastication, swallowing, digestion, tasting and dental hygiene. The nearby auditory tube submucosa also contains microscopic seromucous (tubal or Eustachian tube) glands [5]. The recently introduced molecular imaging modality of positron emission tomography/computed tomography with radio-labelled ligands to the prostate-specific membrane antigen (PSMA[1] PET/CT) can visualize these salivary glands with high sensitivity and specificity [6].

Surprisingly, we observed that PSMA PET/CT also depicted an unknown bilateral structure posterior in the nasopharynx, with

* Corresponding author at: Netherlands Cancer Institute, Plesmanlaan 121, 1066 CX Amsterdam, the Netherlands.
E-mail address: m.valstar@nki.nl (M.H. Valstar).

[1] PSMA= prostate specific membrane antigen.

https://doi.org/10.1016/j.radonc.2020.09.034
0167-8140/

ligand uptake similar to the known major salivary glands (Fig. 1A; Video 1 in the Supplementary material). To our knowledge, this structure did not fit prior anatomical descriptions [5,7]. It was hypothesized that it could contain a large number of seromucous acini, with a physiological role for nasopharynx/oropharynx lubrication and swallowing. This could have clinical relevance in oncology, because high-dose external beam radiotherapy (RT) to salivary glands during treatment for head and neck cancer (HNC) or brain metastasis is known to cause damage (toxicity, e.g. interstitial fibrosis, acinar atrophy). This can result in function loss with xerostomia and dysphagia [8,9]. Affected patients experience impaired food intake, digestion, speech problems and increased risk of caries and oral infections, with significant impact on their quality of life [10–12]. The major salivary glands are therefore regarded as organs-at-risk (OAR) and need to be spared when possible. However, since there are no known localized macroscopic glandular structures posterior in the nasopharynx, this area is not included in currently used prediction models for toxicity, nor spared in RT [13,14].

The identification of previously unnoticed salivary gland structures in the posterior nasopharynx could help to explain and avoid radiation-induced side-effects. We performed a comprehensive multi-perspective study with the objective to confirm the presence of this yet unknown glandular entity, and to assess its anatomical and histological characteristics and clinical relevance in RT.

Materials and methods

Occurrence on molecular imaging

The presence of PSMA-positive tissues in the nasopharynx was evaluated on PSMA PET/CT scans from a retrospective cohort study of 100 consecutively scanned prostate/para-urethral gland cancer patients (from 2017 onwards in NCI and UMCU). Scans were acquired according to routine clinical protocols (Methods 1 in the Supplementary material). The largest cranio-caudal length of the area with uptake was measured on a coronal thick slice and the total tracer uptake in the evaluated region was qualitatively compared with the sublingual glands.

Gland characterization

In a human cadaver study (n = 2), the designated area was dissected as 3 × 3 × 3 cm blocks from bodies retrieved from a body donation program (AUMC, one male, one female). Tissue characteristics were assessed by histochemistry (H&E) and immunohistochemistry (PSMA, alpha-amylase). Immunohistochemistry was performed on a BenchMark Ultra autostainer, Ventana Medical Systems (VMS) (Methods 2 in the Supplementary material). Prostate (for PSMA) and parotid/pancreas (for amylase) samples served as controls. Morphology and anatomical relations were evaluated by 3D-PDF digital reconstruction of anatomy using histological sec-

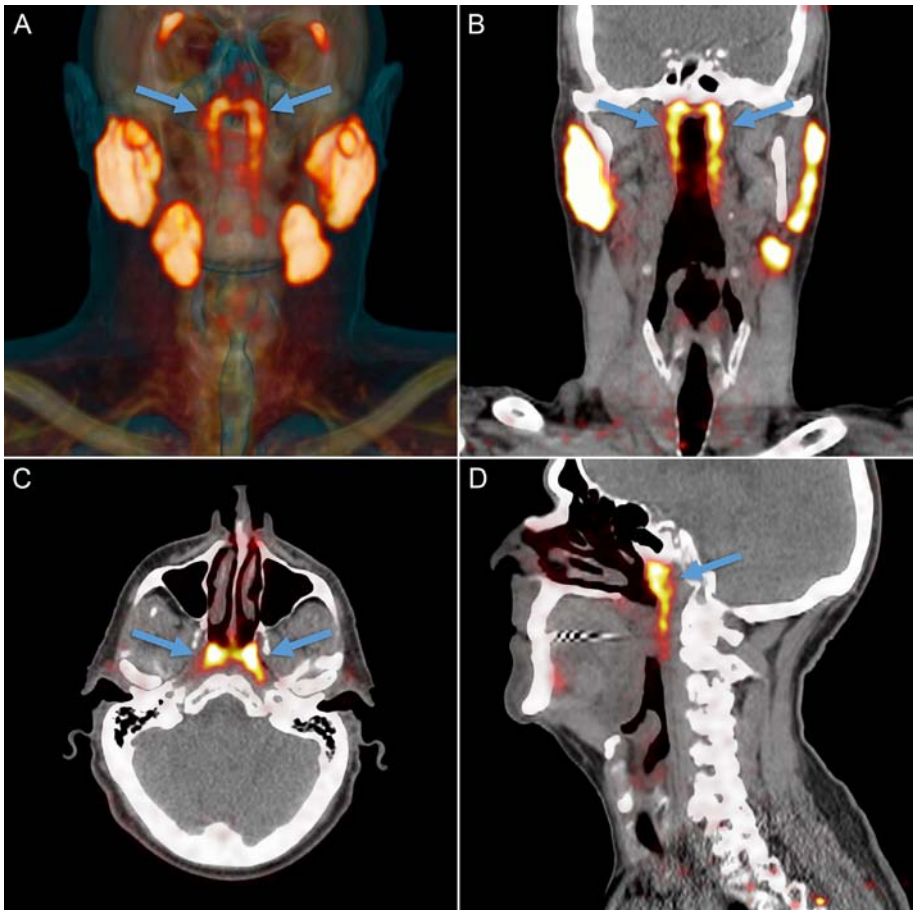

Fig. 1. Projections of PSMA PET/CT. Overview of the salivary gland tissues as seen on PSMA PET/CT. PSMA PET projected as orange signal on reference CT. The known major salivary glands, which include the parotid, submandibular and sublingual glands, all abundantly express PSMA. An unknown structure in the nasopharynx showed similar imaging characteristics (arrows). A 3-dimensional representation of the PSMA PET/CT scan is shown in Video 1 in the Supplementary material. Location and extent of the tubarial glands in a random patient. Shown are coronal (B), axial (C) and sagittal (D) slices at the level of the torus tubarius, of PSMA PET projected as yellow signal on grayscale CT. The glandular structure is visible as PSMA-positive tissue (arrows). The coronal slices also show some parts of the parotid and submandibular glands, which demonstrate similar imaging characteristics.

tions (10 μm, 1/30). The visibility and anatomical features of the gland area on magnetic resonance imaging (Philips Achieve 3T MRI) were assessed in a healthy volunteer (Methods 3 in the Supplementary material).

Clinical relevance in oncology

The relation of RT dose to the designated area with reported toxicity was evaluated using prospectively collected data from patients treated with curative RT, chemoradiation or bioradiation (accelerated RT+cetuximab) for HNC (UMCG March 2007-June 2016; collected with patient consent in a study approved by the ethical committee; https://clinicaltrials.gov: NCT02435576) [14]. All patients received a CT-scan in a personalized immobilization mask in order to define target volumes (including the primary tumor and lymph node metastasis) and OARs (including the major salivary glands, and swallowing muscles, e.g. pharyngeal constrictor muscle-PCM). This treatment planning aimed to deliver the prescribed dose to the target volumes, while sparing the currently considered OARs. For this study, the location and configuration of the newly detected bilateral gland areas were retrospectively defined as additional OARs by deriving anatomical landmarks from the evaluated PSMA PET/CT and MRI scans, while also considering the cadaver-study findings. The cranial border was defined as the skull base caudally of the sphenoid sinus, and the caudal border as the level of the base of the uvula. The lateral border was defined as the skull base at the cranial side and fatty tissue at the caudal side. The anterior border was the skull base cranially and the dorsolateral pharyngeal wall caudally and the posterior border was the prevertebral long musculature. Delineation of this area was performed on the planning CT-scans of all patients, and its' received radiation dose was determined.

Standardized patient-rated and physician-rated toxicities related to treatment of HNC were prospectively collected at 6, 12, 18 and 24 months after treatment, and were scored using the European Organization for Research and Treatment of Cancer Quality of Life Questionnaire - Head and Neck module (EORTC QLQH&N35) and the Common Terminology Criteria for Adverse Events (CTCAE) version 4.0 scores. Multiple imputation was applied to correct for missing data in the follow-up using the MICE package in R [15]. To analyze the association between RT dose to the tubarial gland areas and patient and physician-rated xerostomia and physician-rated dysphagia, multivariable logistic regression analysis was performed to create association models with and without correction for confounding. A two-tailed *P*-value <0.05 was considered statistically significant. Baseline toxicity and mean RT dose to the parotid and submandibular glands were considered as confounders for xerostomia, while for dysphagia, additionally mean RT dose to the pharyngeal constrictor muscle was considered.

Results

All 100 consecutive patients (99 male, one female; median age 69.5; range 53–84) demonstrated a clearly demarcated bilateral PSMA-positive area on PSMA PET/CT. It extended from the skull base downward along the posterolateral pharyngeal wall, on the pharyngeal side of the superior pharyngeal constrictor muscle (PCM-superior), with a PSMA-positive mass predominantly overlaying the torus tubarius (Fig. 1). The median cranio-caudal length of the detected area was 3.9 cm (range 1.0–5.7 cm). The total tracer uptake in the area of interest determined by visual comparison was on average similar to the uptake in the sublingual glands. This was in line with our earlier quantitative evaluation of tracer uptake in the glands of the head and neck [6]. This was consistently more than the uptake in the palate, which is known to contain a high concentration of minor salivary glands.

The dissected area from human cadavers showed a large aggregate of predominantly mucous gland tissue, with multiple macroscopically visible draining duct openings in the dorsolateral pharyngeal wall (Fig. 2). The gland was draped primarily over the torus tubarius, the anatomical structure formed by the cartilage that supports the entrance of the auditory tube. The gland extended caudally to the pharyngeal wall and cranially to Rosenmüllers' fossa. The gland cells showed almost 100% cytoplasmic expression of PSMA with a luminal preference, comparable to the mucous aspect and PSMA-ligand uptake of minor salivary glands in the palate (Fig. 3; Fig. 1 in the Supplementary material). There was no amylase expression in the gland cells consistent with very low numbers of serous acini, similar to the sublingual glands. The 3D histology reconstruction illustrates the anatomical distribution of glandular tissue and draining ducts (Fig. 4; interactive 3D-PDF Fig. 2 in the Supplementary material). MRI images of a healthy volunteer showed a subtle tissue structure with lower signal intensity on the T2 sequence, compatible with glandular tissue, was identified at the expected location of the tubarial gland on the medial side of the torus tubarius (Fig. 3 in the Supplementary material). Small T2-intense dots were present within this tissue structure, which may represent the macroscopic duct openings seen in the cadavers and 3D histology reconstruction.

The characteristics of the 723 evaluable respondents (initial cohort 750), included in the clinical study, are listed in Table 1 in the Supplementary material. The derived gland OAR delineations are illustrated in an anatomical atlas (Fig. 4 in the Supplementary material). The RT dose distribution and delineation of the new gland are shown in Fig. 5 for an example patient.

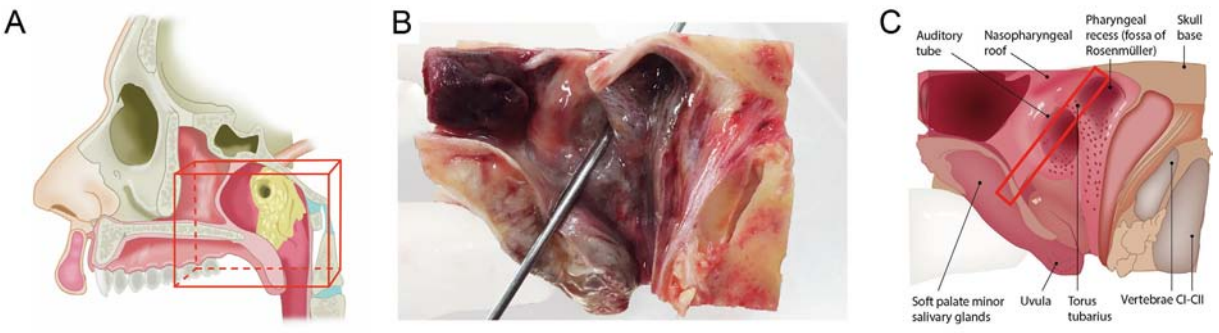

Fig. 2. Anatomy of the torus tubarius area. Macroscopic views of the torus tubarius area. Global anatomical overview with the area of interest in yellow and dissection planes in red (A) with aligned dissection specimen of the right nasopharynx, including a probe showing the auditory tube (B) and annotated graphical overview (C).

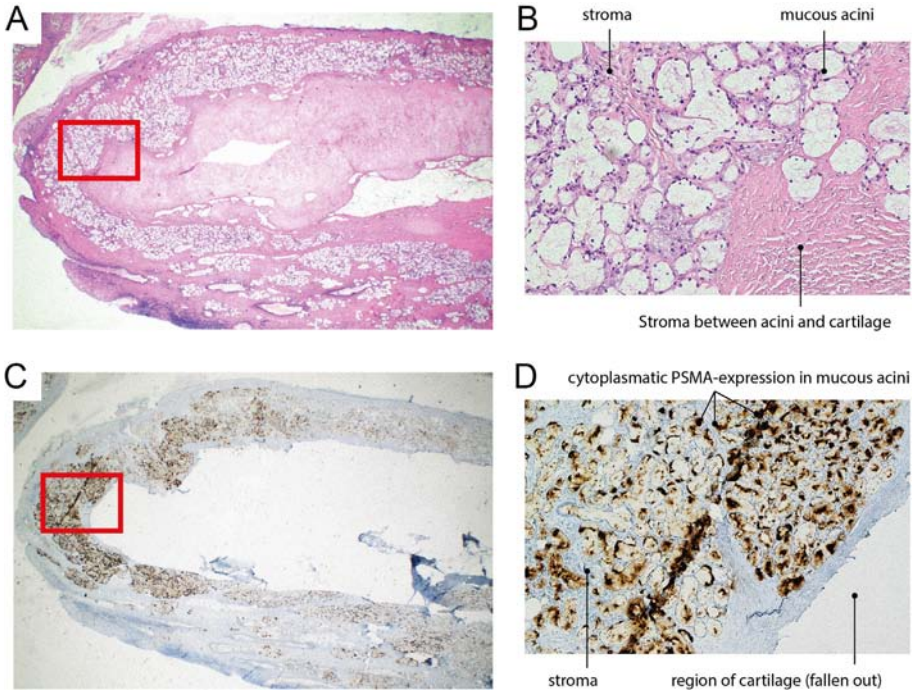

Fig. 3. Torus tubarius with overlying gland histology and immunohistochemistry. Torus tubarius on HE-staining and PSMA-Immunohistochemistry. Histological slides showing the dorsolateral nasopharynx at the level of the torus tubarius (A, 25×) with detail showing an annotated HE-staining (B, 100×). Correlating PSMA staining (C, 25×) with annotated detail showing gland cells covering the cartilage and with the densest collection of mucous PSMA-positive acini overlying the torus tubarius (D, 100×). For an overview with lower magnification see Fig. 1 in the Supplementary material.

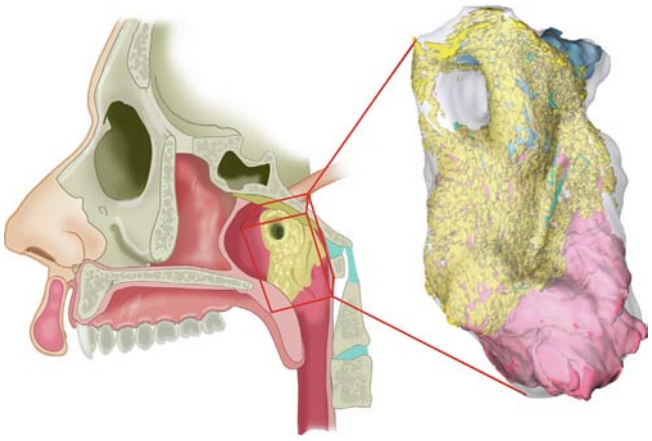

Fig. 4. Newly described gland: Interactive 3D-reconstruction of histological slides. Schematic representation of region of the torus tubarius with overlying gland, in its anatomical setting (left) and as 3D-histology reconstruction (right). The glandular tissue is shown in yellow (acini) and light blue (ducts). This dorsomedial view, demonstrates the relation of the tubarial gland to the underlying torus tubarius cartilage (dark blue) and muscle (pink). An interactive 3D-PDF with the full reconstruction data can be found in Fig. 2 in the Supplementary material.

For crude physician-rated toxicity, the mean RT dose to the new glands was associated at all time points with ≥grade 2 xerostomia (oral intake alterations, e.g. copious water, other lubricants, diet limited to purees and/or soft, moist foods), and with ≥grade 2 dysphagia (symptomatic and altered eating/swallowing) (Table 1 and Table 2 in the Supplementary material). After correction for confounding factors, this association was reduced but still significant at 12- and 24-months. In other words, the effect of RT on dysphagia and xerostomia was explained by RT dose in multiple organs at risk, among which the new glands. However, independently from the dose to the parotid glands as the most relevant OAR, an increase in RT dose to the new glands lead to an increase in toxicity risk (normal tissue complication probability, NTCP) (Fig. 5 in the Supplementary material). For patient-rated xerostomia, the crude association between mean RT dose to the new glands and moderate to severe toxicity was present at all time points, but was reduced and no longer significant after correction for confounding.

Discussion

To our knowledge, this is the first description of paired macroscopic (sero)mucous gland locations in the human posterolateral nasopharyngeal wall, and an indication of their clinical relevance in RT for HNC. Based on its predominant location over the torus tubarius, we propose the name “tubarial glands”. These gland locations were present as macroscopic structures in the PSMA PET/CT scans of all 100 studied individuals, and in two investigated cadavers (one of each gender). Microscopically, they indeed showed salivary gland tissue, highly concentrated bilaterally near the torus tubarius, with macroscopically visible draining duct openings towards the nasopharyngeal wall. High-dose RT to this area lead to significant clinical toxicity. These findings support the identification of the tubarial glands as a new anatomical and functional entity, representing a part of the salivary gland system [3,4,7].

Interpretation of findings

Several factors can explain why these glands have not been noticed previously as macroscopic gland locations. The occurrence of acinar cell groups in the nasopharynx has been reported, but in a spread out pattern in a large region instead of localized tissue in an organized clustered glandular structure [3]. The newly detected tubarial glands involve flat submucosal glandular structures at a poorly accessible anatomical location under the skull base, an area that can only be visualized using nasal endoscopy. The macroscopically visible excretory duct openings may have been noticed, but

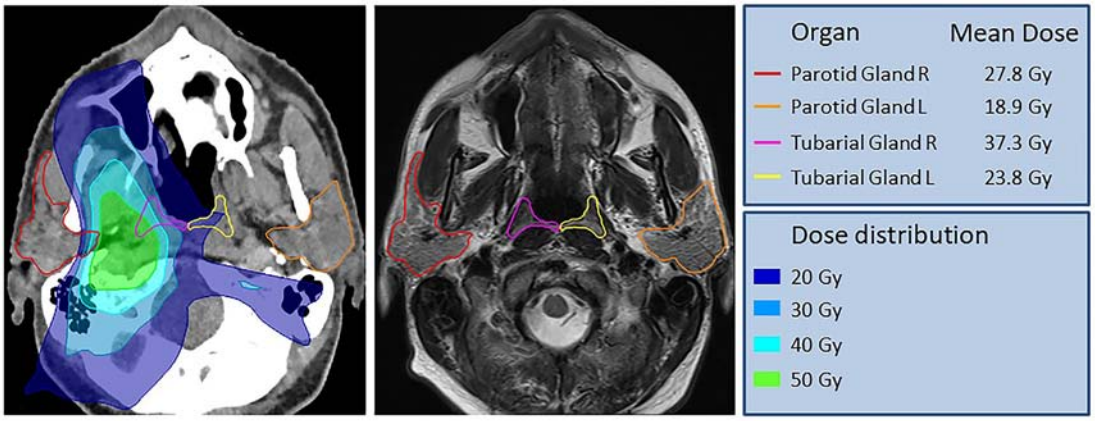

Fig. 5. Radiotherapy evaluation of region of the torus tubarius with overlying gland. Evaluation of radiotherapy dose to the newly described glands overlying the torus tubarius: Axial CT-slice with projected radiation dose distribution as color-wash (left) and MR-slice (right, 3-Tesla, T2-dixon with gadolinium) of a 53-year old patient who received radiotherapy for cT3N1M0 oropharyngeal cancer.

have not been interpreted as part of a larger gland. Conventional imaging modalities (ultrasound, CT, MRI) have never allowed visualization of this submucosal structure and interpretation as a salivary gland, although an indication of its presence may have been visible in various prior functional imaging modalities upon retrospective evaluation [16]. Modern multiparametric MRI imaging could only be used to identify the tissue compartment containing the gland, after analyzing the information provided by PSMA-PET/CT and histology. As a result of these coinciding factors, the discovery depended on the introduction of molecular imaging with radiolabeled PSMA-ligands. This provided the required high sensitivity and specificity for detection of salivary gland cells, with a very high contrast-ratio relative to the surrounding PSMA-negative tissues. In combination with 3D anatomical reconstruction of histological information, this allowed us to realize that these cells in fact form distinctive macroscopic gland locations.

Based on the described anatomical and histological characteristics, and on the demonstrated relation between high-dose RT to the tubarial gland regions and toxicity (xerostomia and dysphagia), we assume the physiological function of the tubarial glands is the moistening and lubrication of the nasopharynx and oropharynx. Although this interpretation of physiology requires confirmation with additional research, it does suggest an opportunity for sparing in RT for patients treated for HNC to avoid toxicity.

One could question whether the tubarial glands should be considered as separate organs, and as major or minor salivary gland locations. However, we think these qualification systems may not be suited and relevant to interpret and appreciate this finding. The accepted definition of an organ is that it consists of more than one kind of tissue, with a definite shape and structure, and performs specific tasks [17]. Indeed, the cadaver study confirmed the presence of a defined structure containing acini and draining ducts, and the association of xerostomia and dysphagia with RT dose in the clinical cohort indicated a specific function that can be disrupted. When compared to the known major salivary glands, the tubarial glands had the most similarities with the sublingual glands based on the predominant mucous acini (hence the negative amylase staining), similar PSMA-ligand uptake, and the presence of multiple draining ducts [6,18]. It can be argued that the tubarial glands do not have a capsule as opposed to the major salivary glands, however the sublingual glands also have an unencapsulated part that consists of 8–30 minor mixed glands [19]. Additionally, the type and frequency of salivary gland tumors that occur in the nasopharynx and sublingual glands seem to be similar, with rare occurrences of benign tumors and adenoid cystic carcinoma as the most frequent malignant tumor [20–26]. As a consequence of these considerations, our interpretation of the tubarial glands could be guided by the classification that is applied to the sublingual glands, and they would qualify as a fourth pair of major salivary glands. On the other hand, the tubarial glands have many similarities with the palatal conglomerate of microscopic glands, which are classified as minor salivary glands. Based on the overlapping spectrum of their characteristics it could be argued that all salivary glands together could be interpreted as a

Table 1
Associations of toxicity and mean dose to the new glands at 12 and 24 months.

	12 Month			24 Month		
	Coef. (gy^{-1})	95% CI	*p*	Coef. (gy^{-1})	95% CI	*P*
Physician rated Xerostomia (≥grade 2)						
Crude	0.047	0.037–0.057	<0.001	0.043	0.033–0.053	<0.001
Corrected (PAR, SM, BL)	0.019	0.005–0.033	0.007	0.018	0.003–0.033	0.02
Physician rated Dysphagia (≥grade 2)						
Crude	0.041	0.033–0.049	<0.001	0.038	0.030–0.046	<0.001
Corrected (PAR, SM, PCM, BL)	0.016	0.001–0.031	0.04	0.02	0.006–0.034	0.006
Patient rated Xerostomia (moderate to severe)						
Crude	0.025	0.018–0.032	<0.001	0.022	0.013–0.031	<0.001
Corrected (PAR, SM, BL)	0.001	−0.011–0.013	0.88	0.001	−0.014–0.016	0.9

Associations of xerostomia and dysphagia with mean dose to newly described glands overlying the torus tubarius. The mean RT dose was associated with grade 2 or higher physician-rated xerostomia and dysphagia at 12 and 24 months post-treatment (For association data including 6 and 18 months, see Table 2 in the Supplementary material). The effect was independent of baseline toxicity and still significant after correction for RT dose in the surrounding OARs that were considered as confounders, i.e., the crude effect was explained by RT dose in multiple OARs among which the new glands had a significant association. The crude association between mean RT dose to the new glands and moderate to severe *patient-rated* xerostomia was present at all time points, but these associations were reduced and not significant after correction for confounders. PAR = parotid; SM = submandibular gland; BL = baseline xerostomia/dysphagia; PCM = pharyngeal constrictor muscle.

continuum, formed by smaller and larger collections of acini that together form a salivary gland system. In this approach, the tubarial glands should not be classified as separate organs or as minor or major salivary glands, and can better be interpreted as macroscopic parts of the composite salivary gland organ system.

Regardless of the classification of the tubarial glands as either a conglomerate of minor glands, a major gland, a separate organ, or as a new part of an organ system, the tubarial glands are macroscopic glandular tissue locations with clinical relevance. Therefore, they require a name that allows unique identification in daily clinical practice. The proposed name tubarial glands is based on their anatomical location, in coherence with the naming strategy for the other macroscopic salivary glands (parotid, submandibular, sublingual). This also prevents confusion with the microscopic tubal glands lining the auditory tube. Other names that were considered included Eustachian or Rosenmüllers' glands, but these did not optimally match the anatomical location, and eponymous medical nomenclature is no longer considered desirable.

Strengths and limitations

The clinical relevance of the tubarial glands was derived from a retrospective evaluation of multiple confounding OARs. Since all salivary glands are situated closely together, they often receive a comparable RT dose in treatment for HNC. As an example, in our data the dose to the parotid glands was highly correlated with the tubarial gland dose, with a correlation coefficient of 0.84. This means that reported xerostomia and dysphagia caused by RT dose to the tubarial glands, also includes a toxicity effect caused by dose to the parotid glands. This phenomenon in statistics, referred to as multicollinearity, complicates measuring a difference in toxicity effects caused by RT to different glands. The same applies to several muscles involved in swallowing in relation to dysphagia. Therefore, a large cohort was required to be able to measure such effects of RT dose to the tubarial glands, after correction for known toxicity effects to adjacent structures. External validity is likely to be warranted by this cohort size and inclusion of unselected consecutive patients. Regarding the internal validity, depending on the time point, 9–37% of the toxicity data are missing (complete) at random (MCAR or MAR) due to death, recurrence, or limited follow-up. A high compliance rate of (88–91%) ensures a low probability of data missing not at random (MNAR).

The association between RT dose to the tubarial glands and crude physician-rated toxicities was present at all time points ($p < .05$). After correction for confounders this association was still present for xerostomia at 12 and 24 months and for dysphagia at 6, 12 and 24 months. The fact that these association after correction were not significant at all four time points can probably be explained by multicollinearity. Similarly, radiation to the oral cavity (which also includes palatal minor glands) might play a role, although RT to this area was not a significantly contributing factor in currently used prediction models [13,14]. More extensive and comprehensive modelling is expected to clarify the influence of multicollinearity. The absence of a significant correlation with patient-rated xerostomia after correction for confounders, may be explained by the inherently higher variability in subjective evaluations of toxicity by patients.

The logical next step seems to be optimization of radiotherapy fields to the tubarial glands as new OARs. Since the PCM superior is close to the tubarial glands, sparing both structures simultaneously seems attractive. Still, we prefer to acquire external validation in an independent dataset, and advise to change clinical protocols only in the setting of continued monitoring of the anticipated clinical benefits. Also, a prospective confirmation of concordance between the tubarial glands as visualised on PSMA PET/CT, with the delineation based on anatomical landmarks is desirable, prior to clinical implementation as a relevant AOR.

We conclude that the human nasopharynx contains previously overlooked bilateral macroscopic salivary glands. Our findings indicate that sparing these tubarial glands could provide an opportunity to prevent side effects from radiotherapy and better maintain patients' quality of life.

Conflict of interest statement

None declared.

Acknowledgements

The authors would like to acknowledge R. Slagter for supplying the medical illustrations; the Core facility Molecular Pathology & Biobanking (NCI) for supplying lab support; J.E. van der Wal for advice on interpretation of histological results; J. Hagoort & C. de Gier–de Vries (Dept. of Medical Biology, Section Clinical Anatomy & Embryology, AUMC) for supplying lab support and 3D-PDF digital histological reconstructions; L. ter Beek (department of radiology, NCI) for technical MRI-support; The Dutch Cancer Society, the Netherlands: Grant number: 10606/2016-2; Maarten van der Weijden Foundation, the Netherlands.

Appendix A. Supplementary data

Supplementary data to this article can be found online at https://doi.org/10.1016/j.radonc.2020.09.034.

References

[1] Holsinger F, Bui D. Anatomy, function and evaluation of the salivary glands. In Myers E, Ferris R, eds. Salivary gland disorders. Springer-Verlag Berlin Heidelberg, 2007; 1-16.
[2] Tuckers A, Ekstroem J, Khosravani N. Embryology and clinical anatomy; Regulatory mechanisms and salivary gland functions. In: Bradley P, Guntinas-Lichius O, editors. Salivary gland disorders and diseases: diagnosis and management. Stuttgart and New York: Thieme; 2011. p. 180.
[3] Tos M. Mucous glands in the developing human rhinopharynx. Laryngoscope 1977;87:987–95.
[4] Richardson MS. Non-neoplastic lesions of the salivary glands. In Thompson L, ed. Head and neck pathology (a volume of foundations in diagnostic pathology). 2nd ed. Elsevier Saunders, 2013; 228.
[5] Tomoda K, Morii S, Yamashita T, Kumazawa T. Deviation with increasing age in histologic appearance of submucosal glands in human eustachian tubes. Acta Otolaryngol 1981;92:463–7.
[6] Klein Nulent TJW, Valstar MH, de Keizer B, et al. Physiological distribution of PSMA-ligand in salivary and seromucous glands of the head and neck on PET/CT. Oral Surg Oral Med Oral Pathol Oral Radiol 2018;125:478–86.
[7] Berger G. Eustachian tube submucosal glands in normal and pathological temporal bones. J Laryngol Otol 1993;107:1099–105.
[8] Price RE, Ang KK, Stephens LC, Peters LJ. Effects of continuous hyperfractionated accelerated and conventionally fractionated radiotherapy on the parotid and submandibular salivary glands of rhesus monkeys. Radiother Oncol 1995;34:39–46.
[9] Radfar L, Sirois DA. Structural and functional injury in minipig salivary glands following fractionated exposure to 70 Gy of ionizing radiation: an animal model for human radiation-induced salivary gland injury. Oral Surg Oral Med Oral Pathol Oral Radiol Endod 2003;96:267–74.
[10] Cheng SCH, Wu VWC, Kwong DLW, Ying MTC. Assessment of post-radiotherapy salivary glands. BJR 2011;84:393–402.
[11] Jellema AP, Slotman BJ, Doornaert P, Leemans CR, Langendijk JA. Impact of radiation-induced xerostomia on quality of life after primary radiotherapy among patients with head and neck cancer. Int J Radiat Oncol Biol Phys 2007;69:751–60.
[12] Wang K, Pearlstein KA, Moon DH, et al. Assessment of risk of xerostomia after whole-brain radiation therapy and association with parotid dose. JAMA Oncol 2018.
[13] Beetz I, Schilstra C, van der Schaaf A, et al. NTCP models for patient-rated xerostomia and sticky saliva after treatment with intensity modulated radiotherapy for head and neck cancer: the role of dosimetric and clinical factors. Radiother Oncol 2012;105:101–6.
[14] Christianen M, van der Schaaf A, van der Laan H, et al. Swallowing sparing intensity modulated radiotherapy (SW-IMRT) in head and neck cancer: clinical

validation according to the model-based approach. Radiother Oncol 2016;118:298–303.
[15] Van Buuren SG-OK. Mice: multivariate imputation by chained equations. R J Stat Software 2011;45:1–67.
[16] Loutfi I, Nair M, Ebrahim A. Salivary gland scintigraphy: the use of semiquantitative analysis for uptake and clearance. J Nucl Med Technol 2003;31:81–5.
[17] Frick H, Leonhardt H, Starck D. Human anatomy. 1st ed. Thieme; 1991.
[18] Korsrud FR, Brandtzaeg P. Characterization of epithelial elements in human major salivary glands by functional markers: localization of amylase, lactoferrin, lysozyme, secretory component, and secretory immunoglobulins by paired immunofluorescence staining.. J Histochem Cytochem 1982;30:657–66.
[19] Bradley P, Guntinas-Lichius O. Salivary gland disorders and diseases: diagnosis and management. 1st ed. Stuttgart and New York: Thieme Publishing Group; 2011.
[20] Guo Z, Liu W, He J. A retrospective cohort study of nasopharyngeal adenocarcinoma: a rare histological type of nasopharyngeal cancer. Clin Otolaryngol 2009;34:322–7.
[21] Andreasen S, Bjørndal K, Agander T, et al. Tumors of the sublingual gland: a national clinicopathologic study of 29 cases. Eur Arch Otorhinolaryngol 2016;273:3847–56.
[22] Pineda-Daboin K, Neto A, Ochoa-Perez V, et al. Nasopharyngeal adenocarcinomas: a clinicopathologic study of 44 cases including immunohistochemical features of 18 papillary phenotypes. Ann Diagn Pathol 2006;10:215–21.
[23] Baradaranfar MH, Dabirmoghaddam P. Endoscopic endonasal surgery for resection of benign sinonasal tumors: experience with 105 patients. Arch Iran Med 2006;9:244–9.
[24] Li T. Minor salivary gland tumors of the nasopharynx. Zhonghua Zhong Liu Za Zhi 1990;12:127–9.
[25] Celik S, Kilic O, Zenginkinet T, et al. Nasopharyngeal pleomorphic adenoma: a rare case report and review of the literature. Case Rep Otolaryngol 2018;2018:1–4.
[26] Spiro R. Salivary neoplasms: overview of a 35-year experience with 2,807 patients. Head Neck Surg 1986;8:177–84.